

2006

# Bowtie Compressor with Novel Capacity Modulation Part 1: Design Description and Model Development

Junhyeung Kim  
*Purdue University*

Eckhard A. Groll  
*Purdue University*

Follow this and additional works at: <http://docs.lib.purdue.edu/icec>

---

Kim, Junhyeung and Groll, Eckhard A., "Bowtie Compressor with Novel Capacity Modulation Part 1: Design Description and Model Development" (2006). *International Compressor Engineering Conference*. Paper 1780.  
<http://docs.lib.purdue.edu/icec/1780>

This document has been made available through Purdue e-Pubs, a service of the Purdue University Libraries. Please contact [epubs@purdue.edu](mailto:epubs@purdue.edu) for additional information.

Complete proceedings may be acquired in print and on CD-ROM directly from the Ray W. Herrick Laboratories at <https://engineering.purdue.edu/Herrick/Events/orderlit.html>

# Bowtie Compressor with Novel Capacity Modulation Part 1: Design Description and Model Development

Jun-Hyeung Kim\*, Eckhard A. Groll

Purdue University,  
School of Mechanical Engineering,  
Ray W. Herrick Laboratories  
West Lafayette, IN. 47907, USA

\*Corresponding Author: phiengineer@gmail.com

## ABSTRACT

A novel refrigeration compressor with an integrated method of capacity modulation for use in domestic refrigerators/freezers is proposed and analyzed here. The compressor is called bowtie compressor due to its two sector-shaped, opposing compression chambers forming a bowtie. The bowtie compressor modulates the cooling capacity by changing the piston stroke without changes of the clearance volume for better thermodynamic efficiency. The new compressor includes a unique off-center-line mechanism so that the piston stroke can be varied without changes in motor rotation. To investigate the feasibility of the proposed compressor, a simulation model has been developed. A detailed description of the bowtie compressor and its simulation model are presented in this paper.

## 1. INTRODUCTION

The compressor of typical domestic refrigerator/freezers is designed to deliver the full cooling capacity at a single speed. Since the cooling capacity of domestic refrigerator/freezers varies throughout their operation, the capacity of the compressor has to be modulated to match the cooling loads.

Conventional compressors are designed to operate at the maximum cooling load. As a result, they cycle on and off in response to the change of the cooling load. This on-and-off operation is not efficient and consumes unnecessary amounts of energy whenever the compressors are turned back on. One way to increase the efficiency of the compressors is to continuously modulate the compressor capacity based on the demand of the cooling load.

A typical method for continuous capacity modulation is variable speed control in which a variable speed motor controls the speed of the piston stroke to match the cooling loads. Theoretical studies by Holdack-Janssen and Kruse (1984), and Zubair and Bahel (1989) reported that variable speed control is the most energy efficient capacity control method at full and part load conditions in comparison to on/off control, hot gas bypass, clearance volume control, and cylinder unloading. In addition, variable speed control introduces the following other advantages: 1) precise thermal control is possible; 2) the reliability of the compressor is improved due to the reduced number of on/off cycles; 3) the response time for set conditions is fast. However, variable speed control is the most expensive method among the other capacity control methods due to the extra cost associated with electronic speed controllers.

In comparison, compressors that do not use variable speed motors, but are able to operate with capacity modulation, can be thought of as cost-effective alternatives to variable speed compressors. The desired features of a compressor with mechanical capacity control are as follows: 1) the thermal efficiency should be as high as that of variable speed motor-driven compressors; 2) the compressor controls the cooling capacity at significantly lower cost than variable speed compressors; 3) the compressor is able to deliver continuous capacity modulation; 4) the compressor structures are simple and reliable.

This paper explores a compressor with novel capacity modulation, which changes the piston stroke by using an inexpensive controller while keeping the same clearance volume for better thermodynamic efficiency. The compressor uses an inexpensive fixed speed motor and does not need a rotational change of the crank shaft. An embodiment of the new compressor, named "Bowtie Compressor," is presented in detail, and its simulation model is discussed in this paper. The Part II paper (Kim and Groll, 2006) presents the model validation, the simulation results, and parametric studies.

## 2 DESCRIPTION OF THE BOWTIE COMPRESSOR

### 2.1 Description of the capacity control

The new compressor concept is shown in Figure 1. The design is based on the Beard-Pennock Variable-Stroke Compressor (Beard and Pennock, 1988), but includes significant modifications. It provides an ideal solution to achieve capacity modulation. The crankshaft rotates counter-clockwise, and the piston rod makes the piston reciprocate axially not linearly. Thus, two compressions take place at the same time. The crankshaft, piston rod, and piston are arranged in such a way that the piston rod is perpendicular to the crankshaft when the piston reaches the top-dead center as shown in the top schematic of Figure 1. The cylinder is placed in the sliding chamber with mechanical springs and pressurized on both ends by the suction and the discharge gases. The cylinder is allowed to slide based on the difference of the two pressure forces. When more capacity is demanded, the difference between the two pressure forces increases. Thus, the force on the right side of the cylinder increases. As a result, the cylinder moves to the left creating a longer stroke which increases the compression volume as shown in the bottom schematic of Figure 2. It has to be noted that the cylinder movement does not create an extra clearance volume. Thus, the capacity modulation is achieved solely by changing the piston stroke.

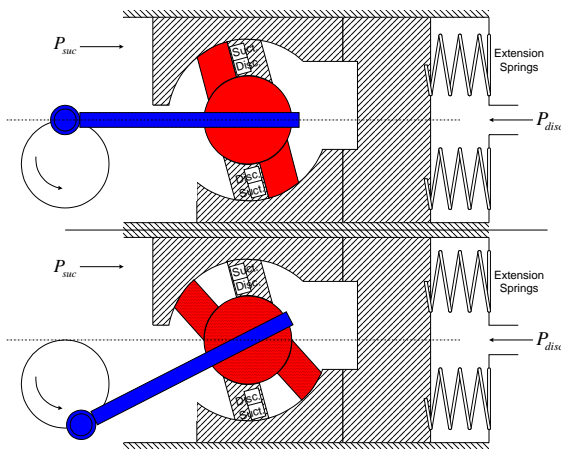


Figure 1: Diagram of the proposed design.

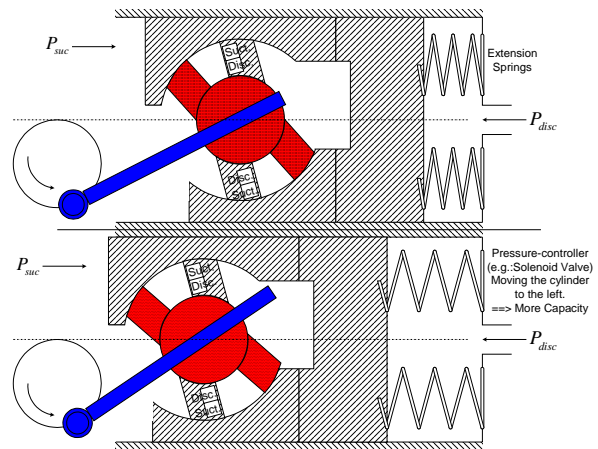


Figure 2: Diagram showing how the piston stroke changes.

Two-step capacity modulation can be realized more easily than multi-step capacity modulation. When more capacity is needed, the high-side pressure is introduced to the right side of the sliding cylinder, and the pressure force moves the cylinder all the way to the left end until it reaches some stopping mechanism. As a consequence, the piston stroke and thus, the capacity is increased. On the other hand, when the normal capacity is required, the introduced pressure is vented out so that the mechanical spring pulls the sliding cylinder back to the right hand side, its initial position. Thus, the stroke and capacity is decreased.

### 2.2 Description of the prototype design

Based on the new compressor concept, a prototype compressor is proposed. Figure 3 shows a cylinder module which consists of six main parts. The module creates two volumetric chambers when all parts are fully assembled as shown in Figure 4. Each chamber produces a volume of  $11 \text{ cm}^3$ . The module is designed in a way that at most  $4.696 \text{ cm}^3$  out of the  $11 \text{ cm}^3$  will be used for the compression process, and the other volume will serve as an intermediate pocket for the incoming refrigerant. Part 4, which can be considered a vane, is a flat rectangular rod with two suction valves on each side. Thus, the suction valves and the rod circumferentially reciprocate together. The discharge valves are installed in Part 3, and are concealed by two pockets on the bottom of Part 5. On the top of Part 5, there are two refrigerant inlets and two outlets. Thus, the refrigerant flows into the compressor from the inlets of Part 5, passes through the pockets in Part 2, the suction valves, the compression chamber, the discharge valves, the pockets in Part 5, and finally flows out of the outlets on Part 5. Part 6 has two rectangular holes so that Part 4 can be inserted in the middle and the connecting rod can be inserted at the bottom. Four panels are put together to linearly guide the cylinder module as shown in Figures 5 and 6. The module is spring-biased so that in default mode, the module is pushed to the right end, and can slide from the right end to the left end by using the actuator. At start-up, the actuator is off so that the compressor operates with a smaller swept volume. When more capacity is

needed, some of the discharge gas is bypassed to activate the actuator. Thus, it results in moving the module to the left end, which creates a larger swept volume.

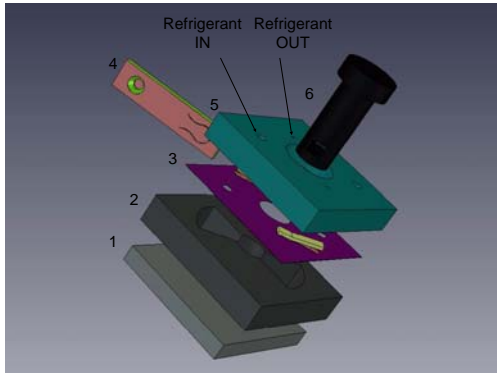


Figure3: Exploded view of the cylinder module.

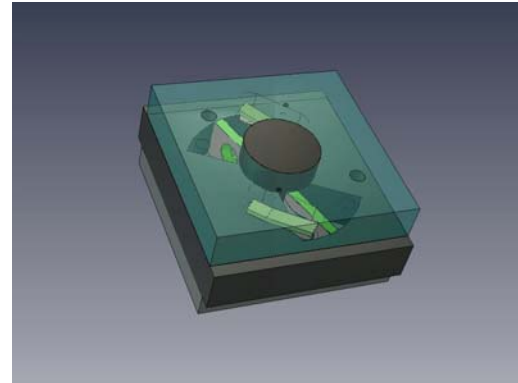


Figure4: Assembled view of the cylinder module.

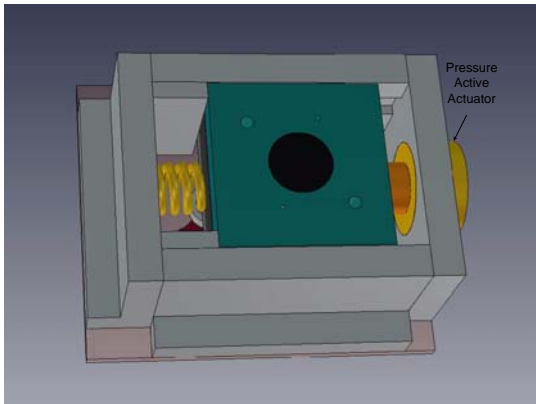


Figure 5: Embodiment of the prototype, the top view.

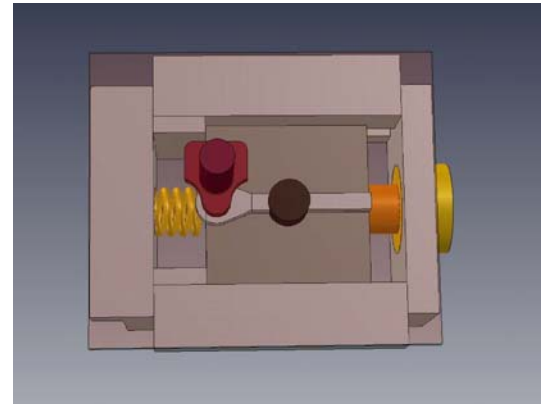


Figure 6: Embodiment of the prototype, the bottom view.

### 3 THEORETICAL ANALYSIS

#### 3.1 Analysis of the kinematics

The analysis of the kinematics of the bowtie compressor is based on the work of Beard and Pennock (1988). Unlike the vector analysis done by Beard and Pennock, a complex analysis is used for the analysis of the kinematics of the bowtie compressor. The complex analysis is more mathematically concise and easier to use than the vector analysis when analyzing the kinematics of a compressor. A vector diagram using an off-center-line mechanism is shown in Figure 7. The eccentricity vector,  $\vec{R}_{01}$ , rotates counter-clockwise. When the eccentricity vector,  $\vec{R}_{01}$ , is at  $90^\circ$ , the vane vector,  $\vec{R}_{25}$ , reaches the top-dead-center, TDC. When the eccentricity vector,  $\vec{R}_{01}$ , further rotates to the point where the angle between the eccentricity vector,  $\vec{R}_{01}$ , and the connecting rod vector,  $\vec{R}_{13}$ , reaches  $90^\circ$ , the vane vector,  $\vec{R}_{25}$ , reaches the bottom-dead-center, BDC. The difference between these two points creates the swept volume of the compressor. The swept volume per unit depth,  $V_{cyl}$ , of the cylinder is determined by:

$$V_{cyl} = \left( \pi r_{25}^2 - \pi r_{24}^2 \right) \frac{\theta_{12}}{2\pi} \quad (1)$$

Using a complex analysis,  $\theta_{12}$  and  $\omega_{12}$  can be calculated as:

$$\theta_{12} = \tan^{-1} \left( \frac{r_{02} \sin \theta_{02} - r_{01} \sin \theta_{01}}{r_{02} \cos \theta_{02} - r_{01} \cos \theta_{01}} \right), \quad \omega_{12} = \frac{1}{\sec^2 \theta_{12}} \left( -r_{01} \frac{d\theta_{01}}{dt} \right) \left[ \frac{r_{02} (\cos \theta_{01} \cos \theta_{02} + \sin \theta_{01} \sin \theta_{02}) - r_{01}}{(r_{02} \cos \theta_{02} - r_{01} \cos \theta_{01})^2} \right] \quad (2)$$

Thus, the speed of the vane end are determined as  $r_{25}\omega_{12}$ .

### 3.2 Analysis of the dynamics

The methodology for the force analysis is based on the work by Beard and Pennock (1988). A force analysis of the proposed design is performed by making the following assumptions: 1) no friction; 2) constant angular velocity of the crankshaft. Three free body diagrams are presented in Figure 8. The diagrams describe the forces on the crank shaft, the connecting rod, the journal shaft and the vane. The pressure forces,  $\vec{F}_{p,shell}$  and  $\vec{F}_{p,cyl}$ , on the vane and journal shaft parts are assumed to be acting on the vane at  $r = (r_{25} + r_{24})/2$ . Using Newton's second law and equations of angular motion, the forces in the free body diagrams are determined.

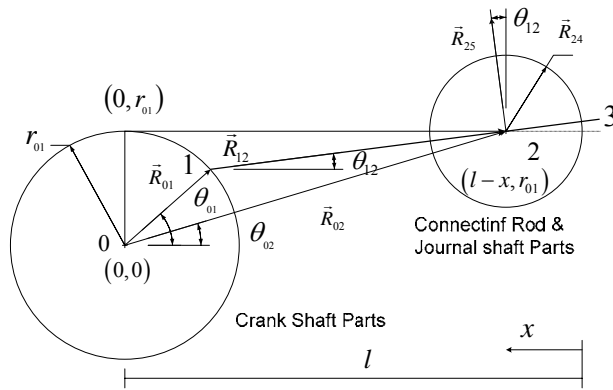


Figure 7: Vector diagram of the proposed design.

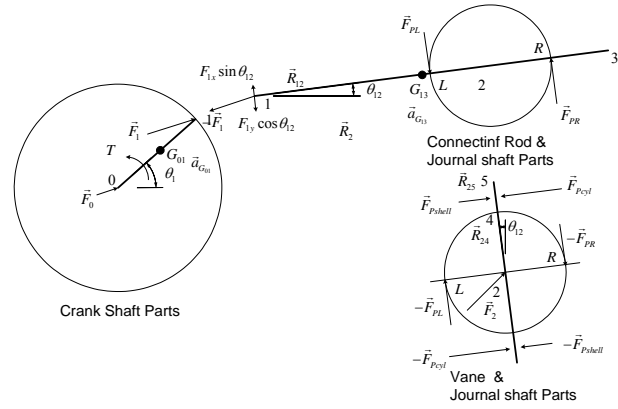


Figure 8: Free body diagrams for the force analysis.

### 3.3 Conservation of mass and energy

The mass change with time inside the cylinder is determined from the conservation of mass as:

$$\frac{dm_{cyl}}{dt} = \frac{dm_{suc}}{dt} + \frac{dm_{leak,in}}{dt} - \frac{dm_{disc}}{dt} - \frac{dm_{leak,out}}{dt} \quad (4)$$

The first law of thermodynamics is applied to derive the temperature change with time in the cylinder (Sun and Ren, 1995). The resulting equation is as follows:

$$\frac{dT_{cyl}}{dt} = \frac{1}{m_{cyl}C_v} \left\{ \frac{dm_{suc}}{dt} (h_{suc} - h_{cyl}) + \frac{dm_{leak,in}}{dt} (h_{leak,in} - h_{cyl}) + T_{cyl} \left( \frac{\partial P_{cyl}}{\partial T_{cyl}} \right)_v \left[ v_{cyl} \frac{dm_{cyl}}{dt} - \frac{dV_{cyl}}{dt} \right] + \frac{dQ_{cyl,wall}}{dt} \right\} \quad (5)$$

There is no heat transfer coefficient available from the literature for the compression process of a bow-tie compressor. However, since the vane is reciprocating circumferentially, the heat transfer coefficient for reciprocating compressors (Annad, 1963) is adopted for the instantaneous heat transfer rate from the refrigerant to the cylinder wall,  $\dot{Q}_{cyl,wall}$  in Eq.(5). Todescat *et al.* (1992) recommended that the heat transfer coefficient is multiplied by a factor of three for a better prediction of the heat transfer rate. The resulting equation is as follows:

$$h(t) = 3 * 0.7 \frac{K(t)}{D_{piston}} \left[ \frac{\rho(t) U_{piston} D_{piston}}{\mu(t)} \right]^{0.7} \quad (6)$$

where  $K(t)$ ,  $\rho(t)$ , and  $\mu(t)$  are thermal conductivity, density, and dynamic viscosity of refrigerant.  $D_{piston}$  is the diameter of the piston, and  $U_{piston}$  is the mean piston velocity(=  $2 \times \text{Stroke} \times \text{rpm} / 60$ ). Modifications are needed in determining the piston diameter and stroke since the swept volume of the vane is not in a cylindrical shape and the stroke of the vane changes with the radius. Thus, a hydraulic diameter and a mean stroke are calculated and used instead. Then, the instantaneous heat transfer from the refrigerant to the cylinder wall is determined as:

$$\dot{Q}_{cyl,wall} = h(t) A(t) [T_{cyl}(t) - T_{wall}] \quad (7)$$

where  $A(t)$  and  $T_{wall}$  are the heat transfer area and the mean wall temperature. It should be noted that the cylinder wall temperature is assumed to be constant. Adair *et al.* (1972) reported that the cylinder wall temperature for a reciprocating compressor changed less than 0.6 K from its time average temperature. Thus, it is reasonable to assume that the cylinder wall temperature is constant.

### 3.4 Dynamic valve model

It is assumed that the gas in the cylinder is at uniform temperature and pressure and that the gas flow through the valve port is isentropic, compressible, and ideal. With these assumptions, the mass flow rates of the discharge and the suction valves can be determined by using the following equation:

$$\dot{m}_{valve} = A_{flow} \sqrt{2\rho_{high} P_{high}} \sqrt{\frac{\gamma}{\gamma-1} \left[ \left( \frac{P_{low}}{P_{high}} \right)^{\frac{2}{\gamma}} - \left( \frac{P_{low}}{P_{high}} \right)^{\frac{\gamma+1}{\gamma}} \right]} \quad (8)$$

The flow area,  $A_{flow}$ , is strongly related to the valve plate lift and can be determined by an experimental test (Soedel, 1972) (Ferreira and Driessen, 1986). However, a theoretical analysis also provides the means of determining the relationship of the valve plate lift and the flow area. It can be recognized that there are two dominant regions when a valve opens and closes dynamically. These regions are a pressure-force dominant region in which the differential pressure force on the valve is the main driving force, and a mass-flux-force dominant region where the pressure forces cancel each other out so that the mass-flux-force is the dominant force as shown in Figure 9. The mass flow rates in each region can be approximated by using the following equations:

$$\begin{aligned} \dot{m}_{valve,p} &= \rho_{cir} V_{cir} A_{cir} \text{ where } \rho_{cir} = f_1(P_{high}, P_{low}) \text{ and } V_{cir} = f_2(P_{high}, P_{low}) \\ &= A_{cir} \sqrt{2\rho_{high} P_{high}} \sqrt{\frac{\gamma}{\gamma-1} \left[ \left( \frac{P_{low}}{P_{high}} \right)^{\frac{2}{\gamma}} - \left( \frac{P_{low}}{P_{high}} \right)^{\frac{\gamma+1}{\gamma}} \right]} \end{aligned} \quad (9)$$

$$\begin{aligned} \dot{m}_{valve,f} &= \rho_{th} V_{th} A_{th} \text{ where } \rho_{th} = f_1(P_{high}, P_{low}) \text{ and } V_{th} = f_2(P_{high}, P_{low}) \\ &= A_{th} \sqrt{2\rho_{high} P_{high}} \sqrt{\frac{\gamma}{\gamma-1} \left[ \left( \frac{P_{low}}{P_{high}} \right)^{\frac{2}{\gamma}} - \left( \frac{P_{low}}{P_{high}} \right)^{\frac{\gamma+1}{\gamma}} \right]} \end{aligned} \quad (10)$$

where  $\dot{m}_{valve,p}$  and  $\dot{m}_{valve,f}$  are the mass flow rate in the pressure-force dominant and the mass-flux-force dominant regions, respectively. It is assumed that most of the flow inside the square box drawn in the pressure dominant region of Figure 9 is stagnant since the leak created by the valve lift is relatively small to the port area. Thus,  $\rho_{cir}$  and  $V_{cir}$  are functions of  $P_{high}$  and  $P_{low}$ . By recognizing that  $\rho_{cir}$  and  $V_{cir}$  are the same as  $\rho_{th}$  and  $V_{th}$  from Eqs. (9) and (10), the transitional valve lift,  $x_{tr}$ , above which the flow area is independent of the valve lift (i.e., the flow area is the port area), can be calculated by letting  $\dot{m}_{valve,p}$  to be the same as  $\dot{m}_{valve,f}$ :

$$\begin{aligned} \rho_{cir} V_{cir} (\pi D_{vavle} x_{tr}) &= \rho_{th} V_{th} \frac{\pi}{4} D_{port}^2 \\ x_{tr} &= \frac{1}{4} \frac{D_{port}^2}{D_{vavle}} \end{aligned} \quad (11)$$

Thus, when the valve lift is less than the transitional valve lift, the valve mass flow rate is determined as:

$$\dot{m}_{valve} = \dot{m}_{valve,p} = \rho_{cir} V_{cir} (\pi D_{vavle} x) \quad (12)$$

When the valve lift is larger than and equal to the transitional valve lift, the valve mass flow rate does not change with the valve lift, and it is calculated as:

$$\dot{m}_{valve} = \dot{m}_{vavle,f} = \rho_{th} V_{th} \frac{\pi}{4} D_{port}^2 \quad (13)$$

The valve plate lift can be determined by analyzing the dynamics of a valve plate. The valve plate is modeled as one-degree of mass and spring (Suefuji and Nakayama, 1980). The natural frequency of the plate spring at the first mode is determined (Blevins, 1979), and the equivalent mass of the plate spring is calculated as:

$$m_{eq} = \frac{k_s}{\omega_{n,1}^2} \tag{14}$$

The main acting forces on the valve plate are a pressure force, a spring force, a drag force and a mass flux force. Other forces, such as the viscous damping force, the oil sticking force and the spring preload force, are neglected due to complexities in identifying them theoretically. For the pressure-force dominant region, the pressure on the left side of the valve obviously decreases from  $P_{high}$  at the center to  $P_{low}$  at the circumference. However, since the valve area is almost the same as the port area, the dominant pressure on the left side of the valve is assumed to be  $P_{high}$ . The governing dynamic equation for the pressure force dominant region is derived as:

$$m_{eq}\ddot{x} + k_s x = (P_{high} - P_{low}) A_{valve} + C_D \frac{1}{2} \rho_{th} V_{th}^2 A_{valve} \tag{15}$$

where  $C_D$  is a drag coefficient for a round plate, which is 1.17. For the mass flux force dominant region, the pressure forces cancel each other out since the control volume is at the same low pressure,  $P_{low}$ . Instead, the mass flux force is added. As a result, the governing dynamic equation is given as:

$$m_{eq}\ddot{x} + k_s x = \rho_{th} (V_{th} - \dot{x})^2 A_{port} + C_D \frac{1}{2} \rho_{th} V_{th}^2 A_{valve} \tag{16}$$

### 3.5 Leakage model

The Ishii *et al.* (1996) leakage model is adopted for the compressor simulation. The main reasons are as follows: 1) fairly good agreements between the experimental data and theoretical results; 2) minimal use of experimental coefficients, which can only be acquired by an actual experiment; 3) the computer calculations are not extensive, i.e., only a small number of iterations are needed.

In this model, it is assumed that the leakage flow is incompressible, viscous, and turbulent. Five possible leakage passages are identified as shown in Figure 10: 1) leakage through the radial clearance,  $\dot{m}_{leak,01}$ ; 2) leakage over the vane,  $\dot{m}_{leak,02}$ ; 3) leakage between the side vane and the journal shaft,  $\dot{m}_{leak,03}$ ; 4) leakage between the journal bearing and the journal shaft,  $\dot{m}_{leak,04}$ ; 5) leakage between the top vane and the journal shaft,  $\dot{m}_{leak,05}$ . Leakage from the valves is not considered because no experimental information is available to determine how the valve clearance changes with changes in pressure difference. In addition, in comparison to the leakage from the vane, the valve leakage is much smaller due to smaller leakage area.

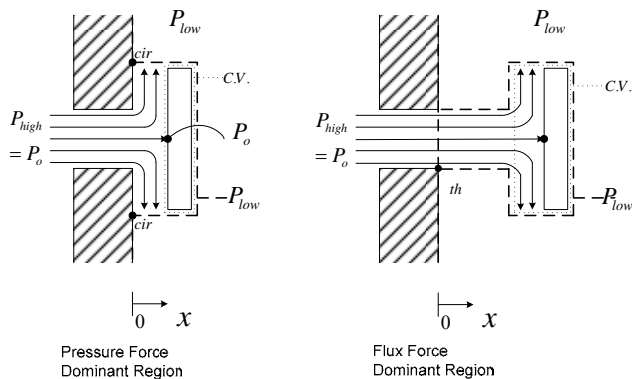


Figure 9: Schematic of a valve.

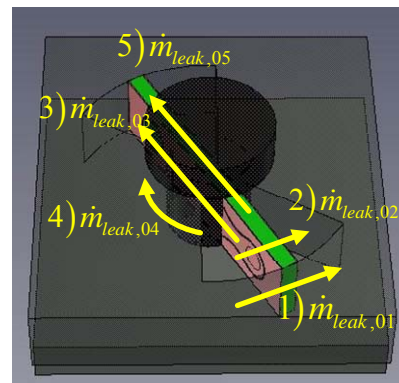


Figure 10: Leakage passages.

### 3.6 Friction loss model

The mechanical friction losses of the bearings are determined using the Reynolds Lubrication Equation with the following assumptions: Newtonian flow, incompressible flow, constant dynamic viscosity, negligible inertia effects, no squeeze motion, and negligible pressure variation across the oil film. The friction analysis is performed on five

parts of the compressor: the vane, the journal shaft in the cylinder block, the sliding bearing, the journal bearing at the end of the eccentricity rod and the crank shaft journal bearing (Kim, 2005).

### 3.7 Overall compressor analysis

An overall energy balance among the motor, the shell, the gas in the shell, the cylinder module, and the ambient air is considered. The overall energy balance model is developed based on the work presented by Chen *et al.* (2002).

Based on the current theoretical model, a simulation code has been developed in Visual C++ 6.0 in conjunction with REFPROP 7.0 for thermal properties. The GNU Scientific Library 1.3 (Galassi *et al.*, 2003) that is compiled for Visual C++ 6.0 is extensively used for numerical calculations, such as solving linear algebra and finding the roots of nonlinear equations. The current simulation model requires the following seven initial guess values: 1) the shell temperature; 2) the refrigerant vapor temperature in the shell; 3) the cylinder wall temperature; 4) the discharge temperature; 5) the compressor cylinder outlet temperature; 6) the oil temperature in the oil sump; 7) the motor RPM. The simulation model continues to iterate until the residuals of each of the seven values are met within an absolute error of 1E-02. Figure 11 shows the flow chart of solving the compressor model starting with the seven initial guess values and an initial step angle.

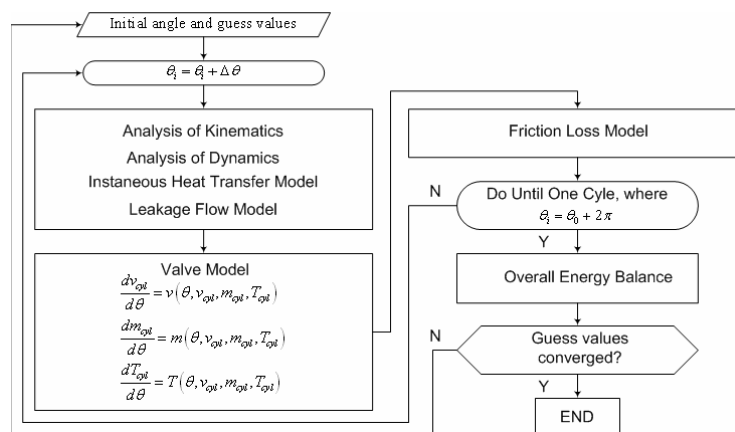


Figure 11: Flow chart for the compressor simulation model.

## 4 CONCLUSION/SUMMARY

A new compressor concept that changes the piston stroke by simple mechanical means while keeping the same clearance volume for better thermodynamic efficiency is proposed here. The new compressor is called bowtie compressor, which uses a unique off-center-line mechanism so that the piston stroke can be varied without changes in clearance volume.

The concept of a bowtie compressor was described in detail. Subsequently, a prototype design of the bowtie compressor was proposed and discussed. The proposed bowtie compressor has some innate features: 1) the cooling capacity can be controlled inexpensively by using a simple on-off solenoid valve without using premium variable speed motors; 2) the compressor always starts with the shorter piston stroke in default mode which results in a smooth startup due to the reduced motor torque; 3) the overall compressor efficiency is improved by keeping the clearance volume constant at all times; 4) continuous capacity modulation can be easily realized by replacing the simple solenoid valve with a more complex valve controller, which leads to further improvement of the overall compressor efficiency.

A simulation model of the proposed compressor was presented to investigate the feasibility of the bowtie compressor. The model includes the following aspects: 1) compression process model to predict the pressure and temperature inside the compression chamber; 2) instantaneous heat transfer model to determine the heat transfer between the compression gas and cylinder walls; 3) leakage model to predict leakage flow rates through different flow paths; 4) frictional loss model to determine the power losses of bearings and due to the shear stress on the vanes and other moving parts; 5) valve model to determine the mass flow rate during the discharge and suction processes; 6) overall energy balance model of the compressor to close the simulation model.

## NOMENCLATURE

$A$	area ( $\text{m}^2$ )	<i>Greek letters</i>	
$A(t)$	time-dependent heat transfer area ( $\text{m}^2$ )	$\gamma$	specific heat ratio
BDC	bottom-dead-center	$\mu(t)$	dynamic viscosity of the gas (Pa sec)
$C_D$	drag coefficient	$\nu$	specific volume ( $\text{m}^3 \text{kg}^{-1}$ )
$C_v$	specific heat at constant volume ( $\text{J kg}^{-1} \text{K}^{-1}$ )	$\omega$	angular velocity ( $\text{sec}^{-1}$ )
$D$	diameter (m)	$\omega_{12}$	angular velocity of the journal shaft ( $\text{sec}^{-1}$ )
$F$	force (N)	$\omega_{n,1}$	natural frequency at the first mode shape ( $\text{sec}^{-1}$ )
$h$	enthalpy ( $\text{J kg}^{-1}$ )	$\rho$	density ( $\text{kg m}^{-3}$ )
$h(t)$	heat transfer coefficient ( $\text{W m}^{-2} \text{K}^{-1}$ )	$\theta$	angle (radian)
$k$	spring stiffness ( $\text{N m}^{-1}$ )	$\theta_{01}$	angle of the eccentricity vector (radian)
$K(t)$	thermal conductivity of the gas ( $\text{W m}^{-1} \text{K}^{-1}$ )	$\theta_{12}$	angle of the connecting rod vector (radian)
$m$	refrigerant mass (kg)	<i>Superscript</i>	
$m_{eq}$	equivalent mass of the plate spring (kg)	$\rightarrow$	vector
$\dot{m}$	mass flow rate ( $\text{kg sec}^{-1}$ )	<i>Subscripts</i>	
$P$	pressure (Pa)	cir	circumference of the valve
$\dot{Q}$	heat transfer rate (W)	cyl	cylinder
$r_{01}$	length of the eccentricity (m)	dis	discharge
$r_{02}$	length of the ground vector (m)	f	flux force
$r_{24}$	length of the journal shaft vector (m)	high	high-side
$r_{25}$	length of the vane vector (m)	in	into the cylinder
$\vec{R}_{01}$	eccentricity vector	leak	leakage
$\vec{R}_{13}$	connecting rod vector	low	low-side
$\vec{R}_{25}$	vane vector	m	mean or average
rpm	rotation per minute	out	out of the cylinder
$t$	time (sec)	p	pressure
$T$	temperature (K)	piston	piston
TDC	top-dead-center	port	port
$U_{piston}$	mean piston speed ( $\text{m sec}^{-1}$ )	shell	in the shell
$V$	velocity ( $\text{m sec}^{-1}$ )	suc	suction
$\forall$	volume ( $\text{m}^3$ )	th	throat of a valve port
$x$	x directional coordinate or x distance (m)	tr	transitional
		valve	valve
		wall	cylinder wall

## REFERENCES

- Adair, R. P., Qvale, E. R., Pearson, J. T., 1972, Instantaneous heat transfer to the cylinder wall in reciprocating compressors, *Proceedings of International Compressor Engineering Conference at Purdue*, p. 521-526.
- Annad, W. J. D., 1963 Heat transfer in the cylinder of reciprocating internal combustion engines, *Institution of Mechanical Engineering*, vol. 177, no. 36, p. 973-996.
- Blevins, R. D., 1979, *Formulas for Natural Frequency and Mode Shape*, Van Nostrand Reinhold Company, New York, NY.
- Chen, Y., Halm, N. P., Groll, E. A., Braun, J. E., 2002, Mathematical modeling of scroll compressors-part II: overall scroll compressor modeling, *International Journal of Refrigeration*, vol. 25, p.751-764.
- Ferreira, R. T. S., Driessen J. L., 1986, Analysis of the influence of valve geometric parameters on the effective flow and force areas, *Proceedings of International Compressor Engineering Conference at Purdue*, p. 632-646.
- Galassi, M., Davies, J., Theiler, J., Gough, B., Jungman, G., Booth, M., Rossi, F., 2003, *GNU Scientific Library Reference Manual (2nd Ed.)*, Network Theory Ltd., ISBN 0954161734.

- Holdack-Janssen, H., Kruse, H., 1984, Continuous and discontinuous capacity control for high speed refrigeration compressors, *Proceedings of International Compressor Engineering Conference at Purdue*, p. 67-75.
- Ishii, N., Bird, K., Sano, K., Oono, M., Iwamura, S., Otokura, T., 1996, Refrigerant leakage flow evaluation for scroll compressors, *Proceedings of International Compressor Engineering Conference at Purdue*, p. 633-638.
- Kim, J.-H., 2005, *Analysis of a bowtie compressor with novel capacity modulation*, Ph.D. Thesis, Purdue University, West Lafayette, IN.
- Kim, J.-H, Groll, E. A., 2006, Bowtie compressor with novel capacity modulation, Part II: Model validation and parametric studies, *Proceedings of International Compressor Engineering Conference at Purdue*, C151.
- Pennock, G. R., Beard, J. E., 1988, The Beard-Pennock variable-stroke compressor, *Proceedings of International Compressor Engineering Conference at Purdue*, p. 599-607.
- Soedel, W., 1972, *Introduction to Computer Simulation of Positive Displacement Type Compressors*, Ray W. Herrick Laboratories, Purdue University, West Lafayette, IN.
- Suefuji, K., Nakayama, S., 1980, Practical method for analysis and estimation of reciprocating hermetic compressor performance, *Proceedings of International Compressor Engineering Conference at Purdue*, p. 15-23.
- Sun, S.-Y., Ren, T.-R., 1995, New method of thermodynamic computation for a reciprocating compressor: computer simulation of working process, *International Journal of Mechanical Science*, vol. 37, no. 4, p. 343-353.
- Todescat, M. L., Fagotti, F., Prata, A. T., Ferreira, R. T. S., 1992, Thermal energy analysis in reciprocating hermetic compressors, *Proceedings of International Compressor Engineering Conference at Purdue*, p. 1419-1428.
- Zubair, S. M., Bahel, V., 1989, Compressor capacity modulation scheme, *Heating/Piping/Air Conditioning*, vol. 61, p. 135-143.
- REFPROP 7.0, 2002, *NIST Standard Reference Database 23: NIST Reference Fluid Thermodynamic and Transport Properties Database (REFPROP): Version 7.0*, National Institute of Standard and Technology, Gaithersburg, Maryland.